Diyala Journal of Engineering Sciences

ISSN 1999-8716
Printed in Iraq

First Engineering Scientific Conference
College of Engineering –University of Diyala
22-23 December 2010, pp. 327-355

A NEW MAPPED INFINITE ELEMENT FOR DYNAMIC ANALYSIS OF SOIL-STRUCTURE INTERACTION PROBLEMS

Mohammed Yousif Fattah
Building and Construction Eng. Dept., University of Technology

ABSTRACT:- In numerical calculations, only a finite region of the foundation radian is analyzed. Unless something is done to prevent the outwardly radiating waves from reflecting from the region's boundaries, errors are introduced into the results. The present work studies such effects, using the finite element method with two types of transmitting boundaries at the edge of the computational grid. The first type is by using mapped infinite element and the second is by using viscous boundaries.

Two types of mapped infinite elements are derived. These types are the 8-noded infinite element extended from that of Zienkiewicz mapped infinite element and the 5-noded coding of mapped infinite element extended from that presented by Selvadurai and Karpurapu in 1988.

The mapping functions and their derivatives of the infinite elements are presented for two cases; the first when the infinite element extending to infinity in the negative ξ direction and in the second case, the infinite element is extending to infinity in the negative η direction.

A dynamic finite-element analysis is carried out for soil-structure interaction problems considering transmitting boundaries. Two types of boundaries are considered: viscous boundaries and mapped infinite elements. The results are compared for three cases; the first one using finite elements only, the second using 5-node and 8-node mapped infinite elements which were added to the finite element code MIXDYN and the third one using viscous boundaries.

In order to check the validity and accuracy of the derived infinite elements in analyzing soil-structure interaction problems considering infinite boundaries, two verification examples are considered for this purpose. The results of the modified program are compared

with the results of other program software called ANSYS representing other types of elements modeling infinite boundaries using viscous boundary method.

It was found that the viscous boundaries are more effective in absorbing the waves resulting from dynamic loads than mapped infinite elements. This is clear when comparing the results of both types with those of transient infinite elements.

INTRODUCTION

Two important characteristics that distinguish the dynamic soil-structure interaction system from other general dynamic structural systems are the unbounded nature and the nonlinearity of the soil medium. Generally, when establishing numerical dynamic soil-structure interaction models, the following problems should be taken into account (Zuo, 2002):

1. Radiation of dynamic energy into the unbounded soil.
2. The hysteretic nature of soil damping.
3. Separation of the soil from the structure.
4. Possibility of soil liquefaction under seismic loads.
5. Other inherent nonlinearities of the soil and the structure.

Details of the analytical techniques also vary according to the nature of the excitation. These can be divided into two broad categories [Wolf, 1988]:

1. Cases where the excitation is applied directly to the structure (e.g. wind, waves, unbalanced masses in rotating machinery, airplane impact or an explosion in the surrounding atmosphere).
2. Situations where the excitation is applied to the structure through the soil (e.g. earthquakes, underground explosion and presupposed elastic waves entering the computational domain or vibrations arising from pile driving, traffic and various other machines).

However, due to the complexity of dynamic soil-structure interaction, numerical modelling of this phenomenon still remains a challenge. Various kinds of analytical formulations and computer programs have been developed to solve the complex problem.

There still exist many difficulties to cover in one model all the problems listed above. Current models usually stress one or several of these problems (Zuo, 2002) .

LOCAL AND NON LOCAL ABSORBING BOUNDARIES

Absorbing boundary conditions can be subdivided in two main classes: local and non-local absorbing boundaries. Figure (1) gives a picture of the concept of localness in

space in the context of discretization with finite element. When the absorbing boundary condition is local in space, the direct coupling of the degrees of freedom is limited to the portion of the boundary modelled by one element. In contrast, an absorbing boundary condition being non local in space directly couples all degrees of freedom of the boundary.

Generally, non-local absorbing boundary conditions are used in the context of frequency-domain analysis because the Fourier transform cancels the non-localness with respect to time. But in frequency domain analysis, the near as well as the far field have to behave linearly. In contrast, local absorbing boundary conditions are used in the context of time domain analysis. Hence they can be applied in nonlinear finite element analysis (near field nonlinear, far field linear) as well. However, because the accurate absorbing boundary conditions of wave dynamics are non-local in space and in time, local absorbing boundary conditions are necessarily approximations.

Examples of non-local absorbing boundaries in the frequency domain are the boundary integral method, the boundary element method, coupled finite element/boundary element method and some types of infinite elements in wave dynamics.

Non local absorbing boundaries in the time domain (the convolution integral approach) are usually derived from the associated frequency domain by way of the inverse Fourier transform.

INFINITE ELEMENTS

It is convenient to classify infinite elements as of static or dynamic type, as the methods needed for the two types are quite different. For static infinite elements, mapped and decay function type can also be used for some dynamic problems.

- **Static Infinite Elements**

The succeeding infinite element formulations have followed two main lines of development. These have been [(Bettess, 1992)]:-

a. Mapping of the element from finite to infinite domain.
b. Using decay functions in conjunction with the ordinary finite element shape function.

- **Mapped Infinite Elements**

Many of the infinite elements proposed have used the idea of mapping, or can be cast in that form. In 1977, Ungless and Anderson used a term of form 1/(1+r) (r is the radial direction) in

three dimensional elasticity applications. Medina and Penzin (1982) adopted the same approach. The first explicit stated mapping was by Beer and Meek (1981), who used a mapping which included the terms ξ_0 :

$$2\,(\xi_j+\tfrac{1}{2})\,\xi \qquad \text{for } \xi < 0 \qquad (1)$$

$$2\,(\xi_j+\tfrac{1}{2})\,\xi/(1-\xi) \qquad \text{for } \xi > 0 \qquad (2)$$

They split the mapping into two parts, that from $\xi = -1$ to $\xi = 0$ and from $\xi = 0$ to $\xi = 1$. The procedure used was fairly complicated.

Beer and Meek also used a standard Gauss-Legendre numerical integration. They found that a simple 2 x 2 integration was beneficial, as a higher order integration tended to make the infinite domain elements too stiff (Beer and Meek, 1981).

Curnier (1983) characterized the two methods (decay function and mapping) as "descent shape function" and "ascent shape function" respectively. It was shown that the two methods can be made equivalent, depending upon the choice of shape function.

Pissanetzky (1984) used a similar approach of Beer and Meek (1981) but he carried out the integration in the infinite domain, and so had to modify the Gauss-Legendre abscissae and weights.

Okabe (1983) gave various possible shape functions for infinite domains, based on what he calls "The generalized Lagrange family for the cube".

The form in which Zienkiewicz mapping was originally given was simplified and systematized by Marques and Owen in 1984, who worked out and tabulated the mapping function for large range of commonly used infinite elements, (Bettess, 1992).

ZIENKIEWICZ MAPPED INFINITE ELEMENTS

There is no doubt that the Zienkiewicz approach (1983) leads to a clarification and simplification of this class of method. The mapping functions and derivatives are given in Table (1) for two-dimensional quadratic serendipity mapped infinite element shown in Figure (2), (Bettess, 1992).

A precisely analogous procedure to derive these mapping functions is described in detail in this paper.

Using the same procedure, mapping functions of the infinite elements will be derived for two cases ; the first when the infinite element extending to infinity in the negative ξ

direction and in the second case, the infinite element is extending to infinity in the negative η direction as shown in Figure (3).

EXTENSION OF TWO-DIMENSIONAL ZIENKIEWICZ MAPPED INFINITE ELEMENTS

For two dimensions, one can derive mapped shape functions to the most usual case that is for an element which is finite in one direction and extends to infinity in the other direction, for example the positive ξ direction. First the mapping functions for the mid-side nodes are derived, see Figure (2). Consider node 8, at ξ = -1 and η = 0.

The mapping function for this node is simply the linear mapping function in ξ multiplied by the quadratic shape function in η that is:

$$M_8 = (1-\eta^2) \times 2/(1-\xi) \tag{3}$$

Now consider node 2 and 6 at ξ = 0 and η = ±1.

The mapping functions for these nodes are simply the quadratic mapping function in ξ multiplied by the appropriate linear shape functions in η, that is :

$$M_2 = (1-\eta)(1+\xi)/2(1-\xi) \tag{4}$$

and

$$M_6 = (1+\eta)(1+\xi)/2(1-\xi) \tag{5}$$

The infinite mapping functions for the nodes at the vertices, ξ = -1 and η = ±1 are now constructed starting with the product of the linear mapping functions in the ξ direction and the linear shape functions in the η direction. Denote these by:

$$\hat{M}_1 = \frac{2}{1-\xi} \times \frac{(1-\eta)}{2} = \frac{(1-\eta)}{(1-\xi)} \tag{6}$$

$$\hat{M}_7 = \frac{2}{1-\xi} \times \frac{(1+\eta)}{2} = \frac{(1+\eta)}{(1-\xi)} \tag{7}$$

These functions are not, however, zero, at the midside nodes. To achieve this, multiples of the midside node mapping functions are now subtracted. The value of the multiple must clearly be the value of the corner mapping functions at the midside nodes.

$$\hat{M}_1(-1,0) = \frac{1}{2} \qquad \hat{M}_7(-1,0) = \frac{1}{2} \tag{8}$$

$$\hat{M}_1(0,-1)=2 \qquad \hat{M}_7(0,1)=2 \tag{9}$$

Hence the final expressions for M_1 and M_7 are :

$$M_1=\hat{M}_1-2M_2-\frac{1}{2}M_8=(-1-\xi+\xi\eta+\eta^2)/(1-\xi) \tag{10}$$

$$M_7=\hat{M}_7-2M_6-\frac{1}{2}M_8=(-1-\xi-\xi\eta+\eta^2)/(1-\xi) \tag{11}$$

The procedure is illustrated in Figure (4).

Following the same procedure we derive:

1. Mapped Shape functions to Elements extending to infinity in the negative ξ direction as shown in Figure (5):

$$M_2=(1-\eta)(1-\xi)/2(1+\xi) \tag{12}$$

$$M_6=(1+\eta)(1-\xi)/2(1+\xi) \tag{13}$$

$$M_4=(1-\eta^2)\times 2/(1+\xi) \tag{14}$$

$$\hat{M}_3=\frac{2}{1+\xi}\times\frac{(1-\eta)}{2}=\frac{(1-\eta)}{(1+\xi)} \tag{15}$$

$$\hat{M}_5=\frac{2}{(1+\xi)}\times\frac{(1+\eta)}{2}=\frac{(1+\eta)}{(1+\xi)} \tag{16}$$

$$\hat{M}_3(1,0)=\frac{1}{2} \qquad \hat{M}_5(1,0)=\frac{1}{2} \tag{17}$$

$$\hat{M}_3(0,1)=2 \qquad \hat{M}_5(0,-1)=2 \tag{18}$$

$$M_3=\hat{M}_3-2M_2-\frac{1}{2}M_4=(1-\eta-1+\xi+\eta-\xi\eta-1+\eta^2)/(1+\xi)$$

$$=(-1+\xi-\xi\eta+\eta^2)/(1+\xi) \tag{19}$$

$$M_5=\hat{M}_5-2M_6-\frac{1}{2}M_4=(1+\eta-1+\xi-\eta+\xi\eta-1+\eta^2)/(1+\xi)$$

$$= (-1+\xi+\xi\eta+\eta^2)/(1+\xi) \qquad (20)$$

2. Mapped shape functions for Element extending to infinity in the negative η direction as shown in Figure (6):

$$M_6 = (1-\xi^2)\times 2/(1+\eta) \qquad (21)$$

$$M_8 = (1-\xi)(1-\eta)/2(1+\eta) \qquad (22)$$

$$M_4 = (1+\xi)(1-\eta)/2(1+\eta) \qquad (23)$$

$$\hat{M}_7 = \frac{2}{(1+\eta)}\times\frac{(1-\xi)}{2} = \frac{(1-\xi)}{(1+\eta)} \qquad (24)$$

$$\hat{M}_5 = \frac{2}{(1+\eta)}\times\frac{(1+\xi)}{2} = \frac{(1+\xi)}{(1+\eta)} \qquad (25)$$

$$\hat{M}_5(0,1) = \frac{1}{2} \qquad \hat{M}_7(0,1) = \frac{1}{2} \qquad (26)$$

$$\hat{M}_5(1,0) = 2 \qquad \hat{M}_7(-1,0) = 2 \qquad (27)$$

$$M_7 = \hat{M}_7 - 2M_8 - \frac{1}{2}M_6 = (1-\xi-1+\eta+\xi-\xi\eta-1+\xi^2)/(1+\eta)$$

$$= (-1+\eta-\xi\eta+\xi^2)/(1+\eta) \qquad (28)$$

$$M_5 = \hat{M}_5 - 2M_4 - \frac{1}{2}M_6 = (1+\xi-1+\eta-\xi+\xi\eta-1+\xi^2)/(1+\eta)$$

$$= (-1+\eta+\xi\eta+\xi^2)/(1+\eta) \qquad (29)$$

The mapping functions and their derivatives for these two cases are derived here and shown in Tables (2) and (3), respectively.

In this paper, this type of mapped infinite element has been added to the finite element models of the computer program (Mod-MIXDYN).

SELVADURAI AND KARPURAPU MAPPED INFINITE ELEMENTS

Selvadurai and Karpurapu in 1986 have extended the scope of mapped type infinite elements to analyze the response of two-phase media such as saturated soils. The technique which uses conventional shape functions and Gauss-Legendre numerical integration was used which makes these elements suitable for implementation in general purpose finite element programs. This element was successfully employed for modeling many geomechanics problems, [Karpurapu, 1988]. Figure (7) illustrates the composite infinite element extends to infinity in ξ direction while table (4) represents their mapping functions, derivatives and shape functions.

Using the same procedure presented in the previous section, derivation of the mapping functions for the infinite elements will be carried out in this study as follows :

case (a) : Infinite element extending to infinity in the negative ξ direction.

case (b) : Infinite element extending to infinity in the negative η direction.

Figure (8) presents the composite infinite element, while tables (5) and (6) represent the mapping functions and the derivatives for cases (a and b).

In this paper, the 5-nodeed serendipity mapped infinite element has also been added to the finite element models of the computer program (Mod-MIXDYN).

APPLICATIONS

In this section, the computer program named "MIXDYN" (Owen and Hinton, 1980) is modified to (Mod-MIXDYN) by adding two extra codes to apply additional type of mapped infinite elements to it. These types are the 8-noded infinite element extended from that of Zienkiewicz mapped infinite element and the 5-noded coding of mapped infinite element extended from that presented by Selvadurai and Karpurapu in 1988.

The program Mod-MIXDYN is coded in Fortran language and implemented on a Pentium-IV personal computer.

In order to check the validity and accuracy of the derived infinite elements in analyzing soil-structure interaction problems considering infinite boundaries, two verification examples are considered for this purpose. The results of the modified program are compared with the results of other program software called ANSYS representing other types of elements modelling infinite boundaries using viscous boundary method.

In the following sections two verification problems are solved. The dynamic analysis parameters and general information for these problems are given in Table (7), (Dawood, 2006).

VERIFICATION PROBLEM NO. (1)

This problem has been previously studied by Yerli et al. (1998). It was solved by three different boundary element method (BEM) formulations. These are frequency domain BEM, time domain BEM, and coupled BEM and FEM in the time domain and using transient infinite elements (TIE). In this system, a dynamic load called Ricker wavelet is considered. The equation of this load in the time domain is:

$$f(t) = f_0 (1 - 2\tau^2) \exp[-\tau^2] \quad (30)$$

where $\tau = (t - t_s)/t_0$

t_s is the time at which the maximum load occurs,

t_0 corresponds to the dominant period of the wavelet, and

f_0 is the amplitude of the load.

In this paper, t_0 was set to $1/\pi$. The time lag t_s was taken equal to $3t_0$:

$t_s = 3/\pi = 0.95$ sec.

The amplitude of the loading is taken as $f_0 = 1 \times 10^{10}$ Newton.

Time history of the loading and the semi-infinite soil system (half-space) are shown in Figure (9), in which P(t) is equal to $f(t)/f_0$.

The problem consists of a layer over rigid bedrock (stratum) as shown in Figure (10). The material properties of both the half-space and the stratum are given in Table (8).

The results are obtained for two cases:

1. Case (1) : Modelling the problem using the program (Mod-MIXDYN) with transmitting boundaries type using five-node mapped infinite element (MIE). The finite and mapped infinite elements mesh for case (1) is shown in Figure (11). The mapped infinite elements are used on the side and bottom boundaries. The length of the infinite elements is chosen to be 200 m after several trials to get results able to be compared with the other cases.
2. Case (2) : Modeling the problem using ANSYS software with transmitting boundaries

type viscous boundaries (VB) using dashpot elements of unit length. Figure (12) shows the finite and dashpot elements mesh for case (2).

Under the action of vertical and horizontal loading, these systems are solved in turn.

Table (9) reports a summary for the mesh information of case (1), while Table (10) gives a summary for the mesh information of case (2).

For comparison, the results obtained from case (1) and case (2) is verified with the results obtained by Yerli et al. (1998) using (TIE) and by Von Estorff et al. (1990) using (BEM) .

Figures (13) to (15) show the time history of the vertical displacement at point A due to vertical load. Figures (16) to (18) show the time history of the horizontal displacement at point A due to vertical load while Figures (19) to (21) show the time history of the horizontal displacement at point A due to horizontal load. Each set of Figures is for cases (1, 2) and the previous studies, respectively.

A comparison between the displacement values of point A at nearly the time when the maximum load occurs for the three cases is shown in Table (11).

Generally, comparing the values and the behaviour of displacements at point A for cases (1) and (2) with the previous studies by Von Estorff et al. (1990) and Yerli et al. (1998), lead to conclusion that case (2) is in good agreement with the previous studies.

The arrival time of the P-wave for Point A is $t_A = OA/V_p = 0.0451$ sec. For $0 \leq t \leq 0.0451$ sec., there is no disturbance at Point A, since none of the waves has reached that point yet, this is clear in all figures.

The responses of the half-space and the stratum are different from each other, since waves are reflected at the soil-bedrock interface and returned back to Point A. As a result of these reflections, the vertical displacements at Point A, due to the vertical load, increase significantly, and the amplitudes of the displacement decrease slowly with increasing t , this is appear clearly in Figures (13) to (15). The vertical displacement on the half-space vanishes after about (2.85 sec.) as shown in Figure (14) for case (2) compared to (2.0 sec.) in Figure (15) while the wave still oscillates in case (1) .

The horizontal displacements at Point A due to the vertical load have the same behaviour as in the previous case, except that the motions have similar magnitudes as shown in Figures (16) to (18).

Finally, from Figures (19) to (21) it is observed that the reflections at the bedrock do not affect considerably the horizontal displacements at the surface.

VERIFICATION PROBLEM NO. (2)

In this case, a half-space with an open rectangular mine shown in Figure (22) is considered. This case was solved by Vardoulakis et al. (1987) using Laplace domain BEM and by Yerli et al. (1998) using transient infinite elements (TIE).

It is assumed that a (15.24) cm thick concrete lining is added on the surface of the open-mined space so that the inside dimensions of the opening remain the same as in the unsupported case. The material properties of the half-space are shown in Table (12).

Under the effect of this loading condition, the plane strain problem is solved by the finite element method with the coupling of finite and infinite elements.

The finite element mesh is shown in Figure (23), while the finite element mesh including infinite elements is shown in Figure (24).

In Figure (25), the finite element mesh with viscous boundaries is drawn. Table (13) lists the required information for the mesh of the problem.

The problem is analyzed using the program (Mod-MIXDYN) and also by the program (ANSYS) for two conditions; fixed and viscous boundaries. Vertical displacements at Points A, B, and C are presented in Figures (26) and (27) adopting viscous boundaries and Figures (28) and (29) adopting fixed boundaries.

For comparison purposes, the results obtained by Vardoulakis et al. (1987) and Yerli et al. (1998) are presented in Figure (30).

It is seen that the vertical displacement of point A is in very good agreement with the results of both Vardoulakis et al. (1987) and Yerli et al. (1998).

For Point B, displacements agree with those of Yerli et al. (1998) rather than those of Vardoulakis et al. (1987).

However, for the displacement at point C, there are big differences between the present results and those of Vardoulakis et al. (1987). But the present results are in good agreement with Yerli et al. (1998) when considering transmitting boundaries. Both the amplitude and the sign of the displacement at point C are different from the results of Vardoulakis et al. (1987).

Because of these discrepancies, this problem was also solved with two alternative methods bz Zerli et al. (1998). The first one is Fourier domain boundary element method BEM developed by Mengi et al. (1994). Using this method, an unsupported case of an

underground opening problem is compared with the infinite elements. The second method is FEM with standard viscous boundaries. It was observed that all of the results by BEM and by FEM with viscous boundary conditions are in good agreement with those obtained by Yerli et al. (1998) formulation and hence with the present formulation too.

CONCLUSIONS

Two types of mapped infinite elements are derived. These types are the 8-noded infinite element extended from that of Zienkiewicz mapped infinite element and the 5-noded coding of mapped infinite element extended from that presented by Selvadurai and Karpurapu in 1988.

The mapping functions and their derivatives of the infinite elements are presented for two cases; the first when the infinite element extending to infinity in the negative ξ direction and in the second case, the infinite element is extending to infinity in the negative η direction.

The following conclusions are drawn:

1) The transmitting boundary absorbs most of the incident energy. The distinct reflections observed in the "fixed boundaries" case disappear in the "transmitted boundaries" case. This is true for both cases of using viscous boundaries or mapped infinite elements.
2) The viscous boundaries are more effective in absorbing the waves resulting from dynamic loads than mapped infinite elements. This is clear when comparing the results of both types with those of transient infinite elements.
3) The results using the present formulation of infinite elements are in good agreement with those of Yerli et al. (1998) when considering transmitting boundaries using transient infinite elements.

REFERENCES

1. G. Beer, and J.L. Meek, ”Infinite Domain Elements”, International Journal for Numerical Methods in Engineering, Vol. 17, P.P. 43-52, 1981.
2. P. Bettess, “Infinite Elements.”, International Journal for Numerical Methods in Engineering, Vol. 11, 1977.
3. P. Bettess, "Infinite Elements”, First Edition, Penshaw Press, 1992.
4. A.Curnier, “A Static Infinite Element”, International Journal for Numerical Methods in Engineering. Vol. 19, p.p. 1479-1488, 1983.

5. S.H. Dawood, "Dynamic Analysis of Soil-Structure Interaction Problems Considering Infinite Boundaries", M.Sc. thesis, University of Technology, Building and Construction Engineering Department, Baghdad, Iraq, 2006.
6. G.R. Karpurapu, "Composite Infinite Element Analysis of Unbounded Two-Phase Media", Computational Mechanics Publications / Adv. Eng. Software, Vol.10, No. 4, 1988.
7. J.M.M.C. Marques, and D.R.J. Owen, "Infinite Elements in Quasi-static Materially Non-linear Problems", Computers and Structures, Vol.18, No. 4, P.P. 739-751, 1984.
8. F. Medina, and J. Penzien, "Infinite Elements for Elastodynamics.", Earthquake Engineering and Structural Dynamics, Vol. 10, 1982.
9. Y. Mengi, A.H. Tanrikulu, and A.K. Tanrikulu, "Boundary Element Method for Elastic Media: An Introduction", METU Press, Ankara, Turkey, 1994.
10. M. Okabe, "Generalized Lagrange Family for the Cube with Special Reference to Infinite Domain Interpolations", Comp. Meth. Appl. Mech. Eng., Vol. 38, No. 2, P.P. 153-168, 1983.
11. D.R.J. Owen and E. Hinton "Finite Elements in Plasticity: Theory and Practice", Pineridge Press Limited, 1980.
12. S. Pissanetsky, "A Simple Infinite Element", Compel, 3, No. 2, Boole Press, Dublin, p.p. 107-114, 1984, (As cited by Bettess, 1992).
13. I.G. Vardoulakis, D.E. Beskos, K.L. Leung, B. Dasgupta and R.L. Sterling, "Computation of Vibration Levels in Underground Space." , International Journal Rock Mech. Min. Sci. and Geomech. Abstracts, Vol. 24, No. 5, P.P. 291-298, 1987.
14. J.P. Wolf., "Soil Structure-Introduction Analysis in Time Domain", Prentice Hall, 1988.
15. H.R. Yerli, B. Temel and E. Kiral, "Transient Infinite Elements for 2D Soil-Structure Interaction Analysis", Journal of Geotechnical and Geo-environmental Engineering, ASCE, Vol. 124. No. 10, P.P. 976-988, October 1998.
16. O.C. Zienkiewicz, C.R.I. Emson, and P. Bettess, "A Novel Boundary Infinite Element", International Journal for Numerical Methods in Engineering", Vol. 19, P.P. 393-404, 1983.
17. D. Zuo, "Numerical Modeling of Dynamic Soil-Structure Interaction during Earthquakes", Term paper, from the Internet, 2002.

Table (1): Serendipity eight-node two dimensional infinite element, (Bettess, 1992) The mapping functions and derivatives.

Node , i	ξ_i	η_i	*Mi*	$\partial Mi/\partial\xi$	$\partial Mi/\partial\eta$
6	0	1	$(1+\xi)(1+\eta)\ /2(1-\xi)$	$(1+\eta)/(1-\xi)^2$	$(1+\xi)/2(1-\xi)$
7	-1	1	$(-1-\xi-\xi\eta+\eta^2)\ /(1-\xi)$	$(-2-\eta+\eta^2)/(1-\xi)^2$	$-\xi+2\eta/(1-\xi)$
8	-1	0	$2(1-\eta^2)/\ (1-\xi)$	$2(1-\eta^2)/(1-\xi)^2$	$-4\eta/(1-\xi)$
1	-1	-1	$(-1-\xi+\xi\eta+\eta^2)\ /(1-\xi)$	$(-2+\eta+\eta^2)/(1-\xi)^2$	$(\xi+2\eta)/(1-\xi)$
2	0	-1	$(1+\xi)(1-\eta)\ /2(1-\xi)$	$(1-\eta)/(1-\xi)^2$	$-(1+\xi)/2(1-\xi)$

Table (2): Serendipity eight-node two dimensional infinite element extending to infinity representing case a. The mapping functions and derivatives for element extending to negative ξ direction, as derived in this study.

Node, i	ξ_i	η_i	*Mi*	$\partial Mi/\partial\xi$	$\partial Mi/\partial\eta$
2	0	-1	$(1-\xi)(1-\eta)\ /2(1+\xi)$	$-(1+\eta)/(1+\xi)^2$	$-(1-\xi)/2(1+\xi)$
3	1	-1	$(-1+\xi-\xi\eta+\eta^2)\ /(1+\xi)$	$(2-\eta-\eta^2)/(1+\xi)^2$	$-\xi+2\eta/(1+\xi)$
4	1	0	$2(1-\eta^2)/\ (1+\xi)$	$-2(1-\eta^2)/(1+\xi)^2$	$-4\eta/(1+\xi)$
5	1	1	$(-1+\xi+\xi\eta+\eta^2)\ /(1+\xi)$	$(2+\eta-\eta^2)/(1+\xi)^2$	$(\xi+2\eta)/(1+\xi)$
6	0	1	$(1-\xi)(1+\eta)\ /2(1+\xi)$	$(1+\eta)/(1+\xi)^2$	$(1-\xi)/2(1+\xi)$

Table (3): Serendipity eight-node two dimensional infinite element extending to infinity representing case b. The mapping functions and derivatives element extending to negative η direction, as derived in this study.

Node, i	ξ_i	η_i	*Mi*	$\partial Mi/\partial\xi$	$\partial Mi/\partial\xi$
4	1	0	$(1+\xi)(1-\eta)\ /2(1+\eta)$	$(1-\eta)/2(1+\eta)$	$(1-\eta)/2(1+\eta)$
5	1	1	$(-1+\eta+\xi\eta+\xi^2)\ /(1+\eta)$	$(\eta+2\xi)/(1+\eta)$	$2-\xi^2+\xi/(1+\eta)^2$
6	0	1	$2(1-\xi^2)/\ (1+\eta)$	$-4\xi/(1+\eta)$	$-2(1-\xi^2)/(1+\eta)^2$
7	-1	1	$(-1+\eta-\xi\eta+\xi^2)\ /(1+\eta)$	$(-\eta+2\xi)/(1+\eta)$	$2-\xi-\xi^2/(1+\eta)^2$
8	-1	0	$(1-\xi)(1-\eta)\ /2(1+\eta)$	$-(1-\eta)/2(1+\eta)$	$-(1-\xi)/(1+\eta)^2$

Table (4): Mapping and shape functions for composite mapped infinite element, (Karpurapu,1988).

Mapping functions and derivatives.

Node, i	2-noded Superparametric Mi	5-noded Serendipity isoparametric Mi	5-noded $\partial Mi/\partial\xi$	5-noded $\partial Mi/\partial\eta$
1	$-\xi(1+\eta)/\ (1-\xi)$	$-\xi\eta(1+\eta)/\ (1-\xi)$	$-\eta(1+\eta)/\ (1-\xi)^2$	$-\xi(1+2\eta)/(1-\xi)$
2	$-\xi(1-\eta)/\ (1-\xi)$	$\xi\eta(1-\eta)/\ (1-\xi)$	$\eta(1-\eta)/\ (1-\xi)^2$	$\xi(1-2\eta)/(1-\xi)$
3	$(1+\xi)(1-\eta)\ /2(1-\xi)$	$-2\xi(1-\eta^2)/\ (1-\xi)$	$-2(1-\eta^2)/\ (1-\xi)^2$	$4\xi\eta/(1-\xi)$
4	$(1+\xi)(1+\eta)\ /2(1-\xi)$	$(1+\xi)(1-\eta)\ /2(1-\xi)$	$(1-\eta)\ /(1-\xi)^2$	$-(1+\xi)/2(1-\xi)$
5		$(1+\xi)(1+\eta)\ /2(1-\xi)$	$(1+\eta)\ /(1-\xi)^2$	$(1+\xi)/2(1-\xi)$

Shape Functions

Node, i	2-noded Superparametric Ni	5-noded Serendipity isoparametric Ni
1	$(1-\xi)(1+\eta)/4$	$(1-\xi)(1+\eta)/4-(1-\xi^2)(1+\eta)/4-(1-\xi)(1-\eta^2)/4$
2	$(1-\xi)(1-\eta)/4$	$(1-\xi)(1-\eta)/4-(1-\xi)(1-\eta^2)/4-(1-\xi^2)(1-\eta)/4$
3		$(1-\xi)(1-\eta^2)/2$
4		$(1-\xi^2)(1-\eta)/2$
5		$(1-\xi^2)(1+\eta)/2$

Table (5): Mapping functions for 5-noded serendipity mapped infinite element and their derivatives for case (a) as derived in this study.

Node, i	ξ_i	η_i	5-noded serendipity Mi case a.	5-noded $\partial Mi/\partial\xi$	5-noded $\partial Mi/\partial\eta$
1	1	1	$\xi\eta(1+\eta)/\ (1+\xi)$	$\eta(1+\eta)/\ (1+\xi)^2$	$\xi(1+2\eta)/(1+\xi)$
2	1	-1	$-\xi\eta(1-\eta)/\ (1+\xi)$	$-\eta(1-\eta)/\ (1+\xi)^2$	$-\xi(1-2\eta)/(1+\xi)$
3	1	0	$2\xi(1-\eta^2)/\ (1+\xi)$	$2(1-\eta^2)/\ (1+\xi)^2$	$-4\xi\eta/(1+\xi)$
4	-1	-1	$(1-\xi)(1-\eta)\ /2(1+\xi)$	$(-1+\eta)\ /(1+\xi)^2$	$-(1-\xi)/2(1+\xi)$
5	-1	1	$(1-\xi)(1+\eta)\ /2(1+\xi)$	$-(1+\eta)\ /(1+\xi)^2$	$(1-\xi)/2(1+\xi)$

Table (6): Mapping functions for 5-noded serendipity mapped infinite element and their derivatives for case (b) as derived in this study.

Node, i	ξ_i	η_i	5-noded serendipity Mi case b	5-noded $\partial Mi/\partial\xi$	5-noded $\partial Mi/\partial\eta$
1	1	1	$\xi\eta(1+\xi)/\ (1+\eta)$	$\xi(1+\xi)/\ (1+\eta)^2$	$\eta(1+2\xi)/(1+\eta)$
2	-1	1	$-\xi\eta(1-\xi)/\ (1+\eta)$	$-\xi(1-\xi)/\ (1+\eta)^2$	$-\eta(1-2\xi)/(1+\eta)$
3	0	1	$2\eta(1-\xi^2)/\ (1+\eta)$	$2(1-\xi^2)/\ (1+\eta)^2$	$-4\xi\eta/(1+\eta)$
4	-1	-1	$(1-\xi)(1-\eta)\ /2(1+\eta)$	$(-1+\xi)/\ (1+\eta)^2$	$-(1-\eta)/2(1-\eta)$
5	1	-1	$(1+\xi)(1-\eta)\ /2(1+\eta)$	$(-1-\xi)/\ (1+\eta)^2$	$(1-\eta)/2(1-\eta)$

Table (7): General information for the three verification problems.

Type of the problems		Plane strain
Displacement analysis		Elastic analysis
Newmark integration parameters	δ	0.5
	α_n	0.25
Damping parameters	α	0
	β	0.00075
Tolerance		0.0001
Max No. of iterations		55

Table (8): Material properties for problem No. (1).

Property	Value
Modulus of elasticity, E	2.66×10^8 N/m^2
Poisson's ratio, μ	0.33
Density, γ	2,000 kg/m^3

Table (9): Meshes information for problem No. (1).

Type of information	Mod-MIXDYN Infinite +Finite Elements	
	Half-Space	Stratum
No. of nodes	702	683
No. of elements F.E	200	200
Infinite elements	40	20
Dashpot elements	-	-
Total No. of nodal points with fixed degrees of freedom	44	44
Total No. of time steps	325	325
Time step length (sec.)	0.01	0.01

Table (10): Meshe information for problem No. (1), solved by ANSYS showing both half space and stratum.

Type of information	ANSYS (Viscous boundaries)	
	Half-Space	Stratum
No. of nodes	763	701
No. of elements F.E	200	200
Infinite elements	-	-
Dashpot elements	82	40
Total No. of nodal points with fixed degrees of freedom	44	44
Total No. of time steps	325	325
Time step length (sec.)	0.01	0.01
C_t (kN-sec.)/m^3	451.59	451.59
C_n (kN-sec.)/m^3	729	729

Table (11): A comparison between the displacement values of point A at nearly the time when the maximum load occurs for the three cases.

			Transmitting boundary description					
			Transient infinite elements (Yerli et al., 1998)		Case (1) Mapped infinite elements		Case (2) Viscous boundary using dash-pot elements	
Load type	Case	Displ. direction	Displ. ($m*10^{-7}$)	@ Time (sec.)	Displ. ($m*10^{-7}$)	@ Time (sec.)	Displ. ($m*10^{-7}$)	@ Time (sec.)
Vertical load	Half-Space	Uy	30.0	1.14	26.1	1.17	31.0	1.17
	Stratum		46.0	1.14	49	1.2	47.4	1.19
Vertical load	Half-Space	Ux	7.5	1.05	13.8	1.04	11.7	1.09
	Stratum		10	1.05	14.0	1.08	13.6	1.09
Horizontal load	Half-Space	Ux	35.0	1.10	44.0	1.12	36.6	1.07
	Stratum		40.0	1.10	44.0	1.12	37.6	1.12

Table (12): Material properties of the soil and concrete for problem No. (2) (from Yerli et al., 1998).

Material Properties	Soil	Concrete
Shear modulus, G (N/m^2)	470.24×10^6	10622.0×10^6
Poisson's ratio, μ	0.10	0.17
Density, □ (kg/m^3)	2048	2263

Table (13): Mine problem No. (2) mesh information.

Type of information	Mod-MIXDYN		ANSYS Viscous boundaries
	Fixed bounbaries	Infinite elements	
No. of nodes	696	740	828
No. finite of elements	208	208	208
Infinite elements	-	43	-
Dashpots	-	-	88
Total No. of nodal points with fixed degrees of freedom	44	44	44
Total No. of time steps	375	375	375
Time step length (sec.)	0.0002	0.0002	0.0002

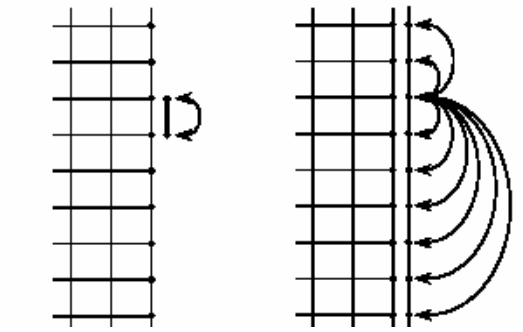

Fig. (1): The coupling of local (left) and non-local (right) absorbing boundary conditions with respect to space.

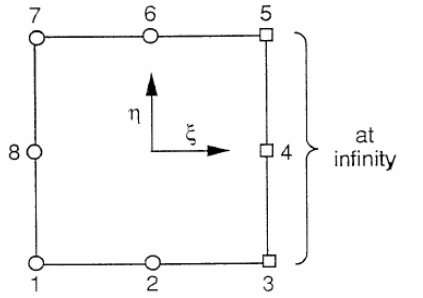

Fig. (2): Serendipity infinite element nodal numbering, element extending to infinity at positive ξ direction, (Bettess, 1992).

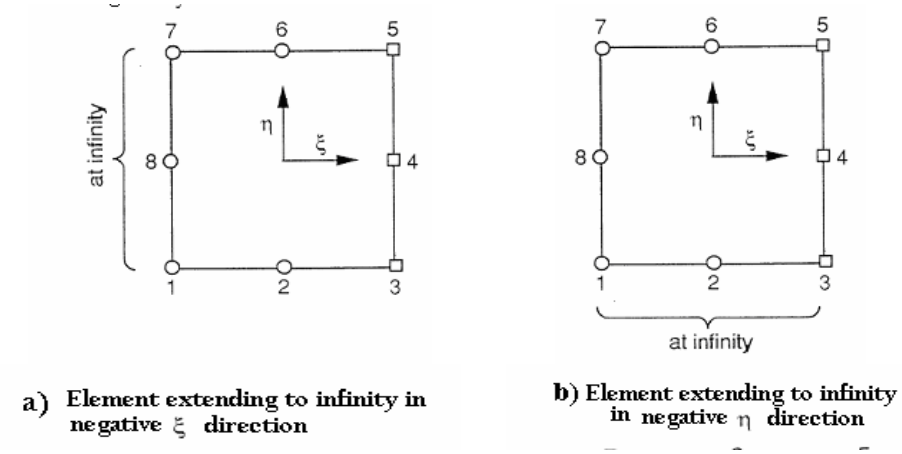

Fig. (3): Serendipity infinite element nodal numbering, element extending to:
a) Negative ξ direction. b) Negative η direction

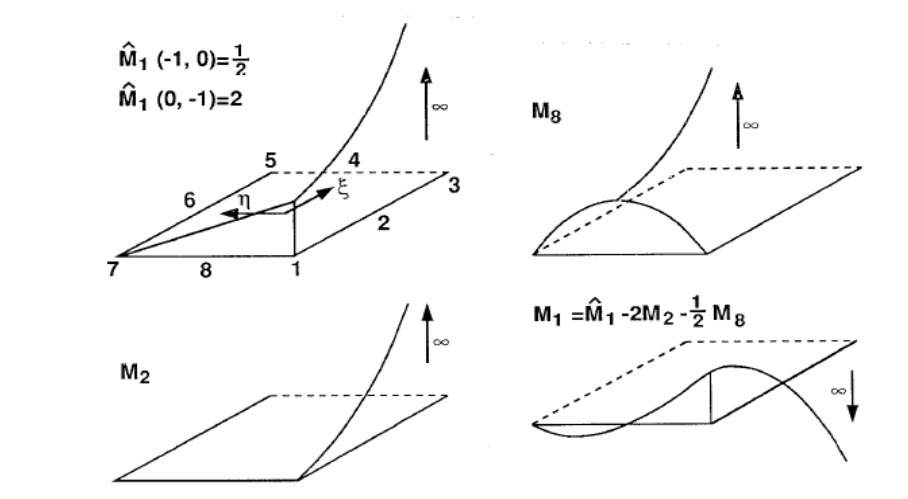

Fig. (4): construction of Serendipity infinite mapping function .

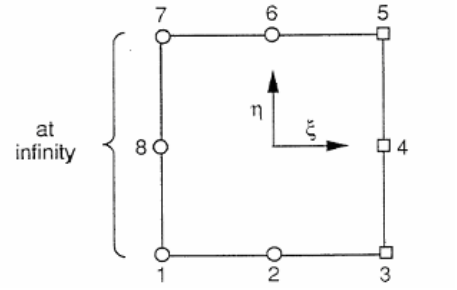

Fig. (5): Serendipity infinite element nodal numbering (Negative ξ direction).

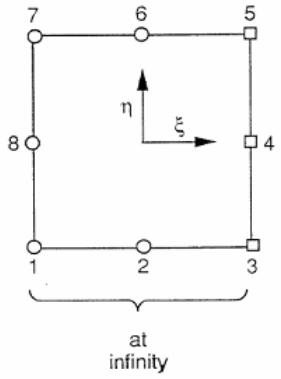

Fig. (6): Serendipity infinite element nodal numbering (Negative η direction).

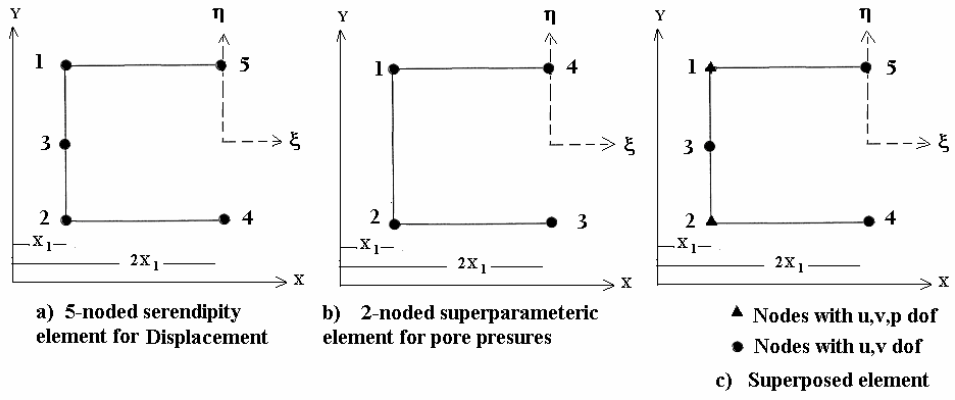

Fig. (7): The composite infinite element, (Karpurapu, 1988).

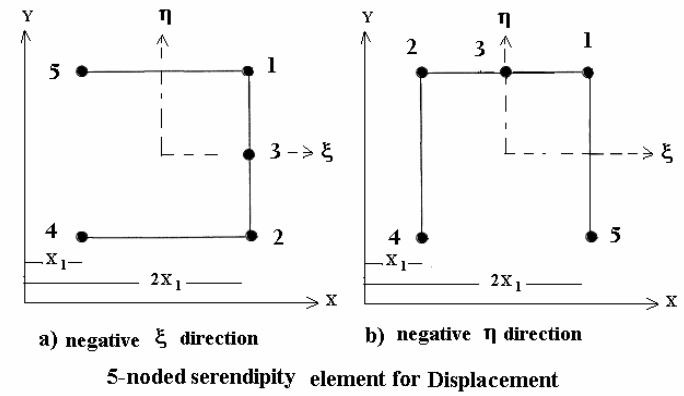

Fig. (8): The composite infinite elements proposed in this study cases (a) and (b) .

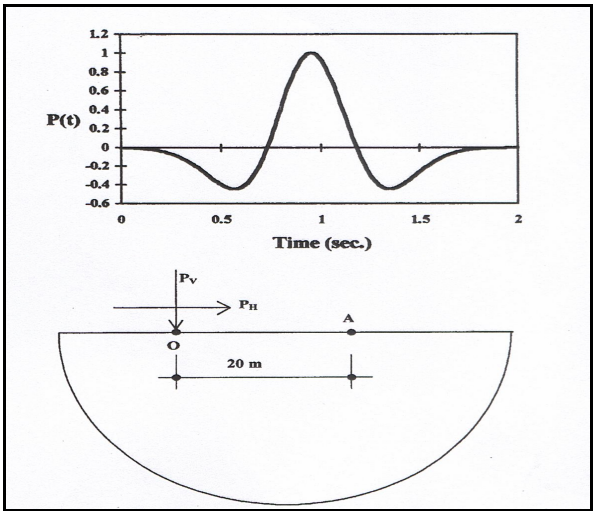

Fig. (9) : Ricker wavelet loading and semi-infinite half-space system, (Yerli et al., 1998).

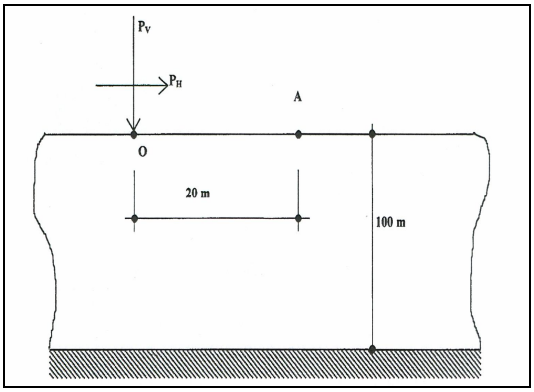

Fig. (10) : Layer over rigid bedrock (stratum) , (Yerli et al., 1998).

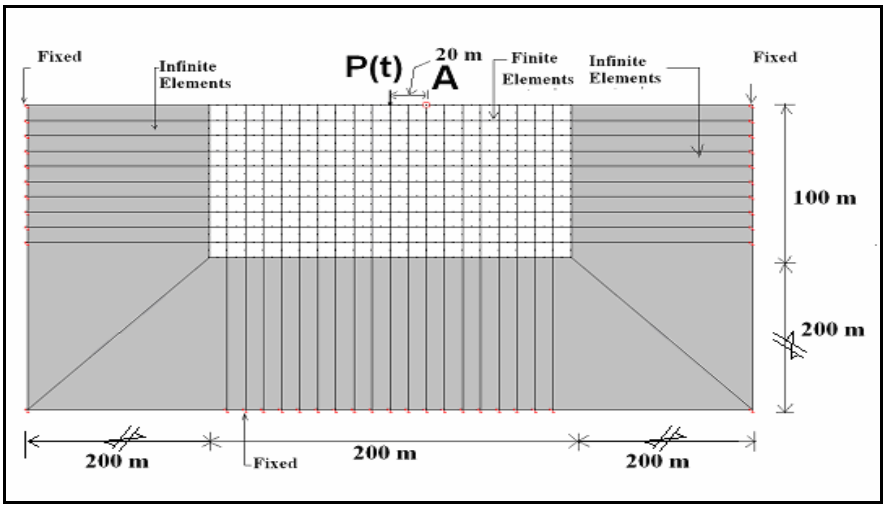

(a) Half-Space finite and infinite elements mesh.

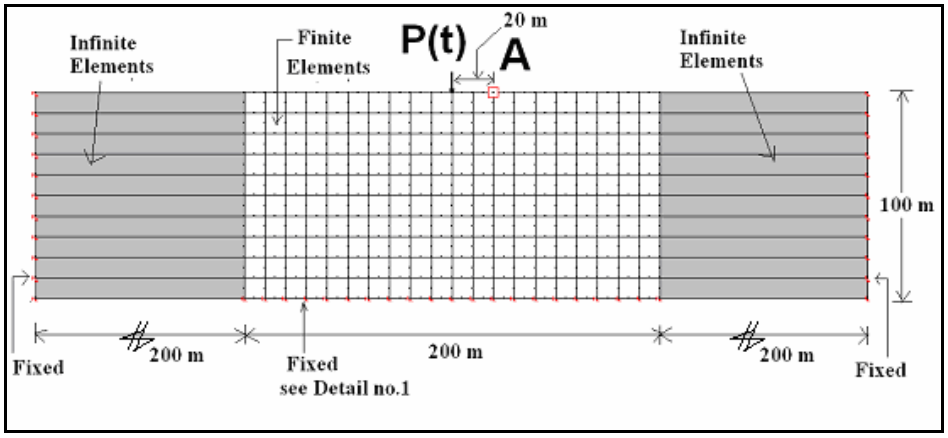

(b) Stratum of finite and infinite elements mesh.

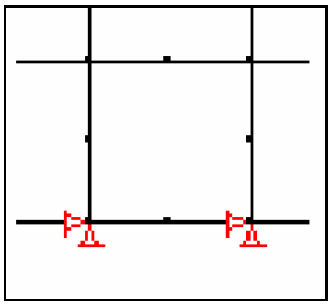

Fig. (11): Half-space and stratum finite and infinite elements meshes for problem No.(1), including fixed detail.

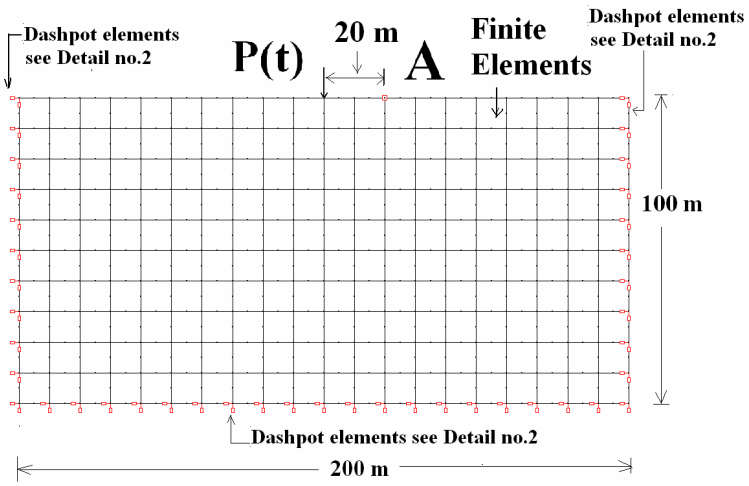

(a) Half-space finite and dashpot elements mesh.

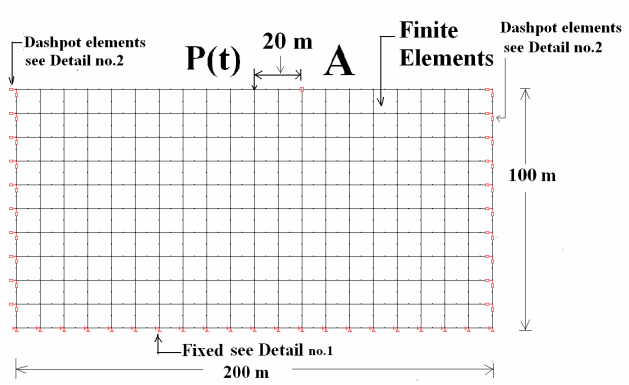

(b) Stratum finite and dashpot elements mesh.

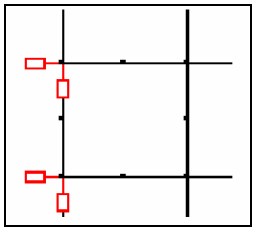

Detail no. 2 : Dashpot elements (Viscous oundaries)

Fig. (12): Half space and Stratum meshes for problem No. (1), including dashpot elements detail.

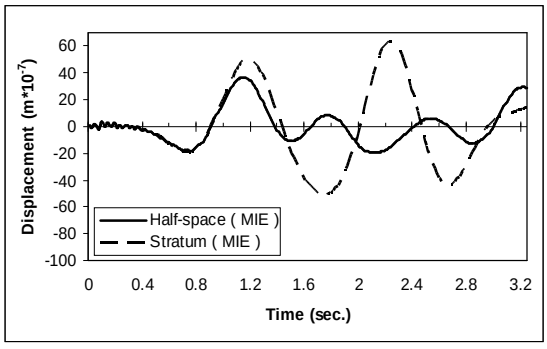

Fig. (13): Time history of vertical displacements at point A due to vertical load predicted by Mod-MIXDYN (MIE).

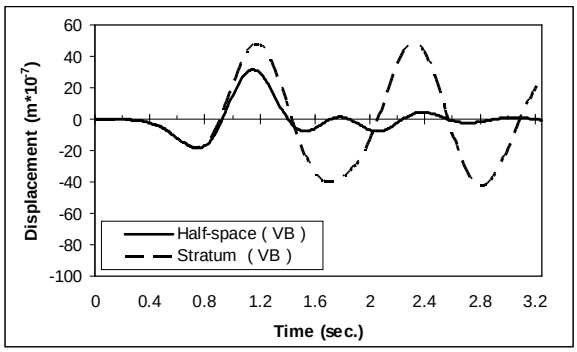

Fig. (14): Time history of vertical displacements at point A due to vertical load predicted by ANSYS using (VB).

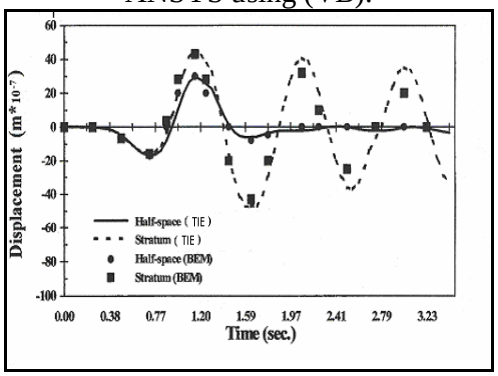

Fig. (15): Time history of vertical displacements at point A due to vertical load,(Yerli et al., 1998).

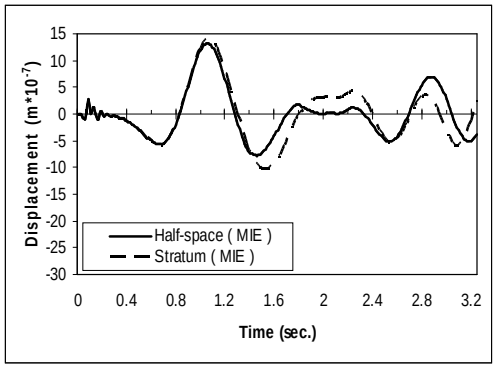

Fig. (16): Time history of horizontal displacements at point A due to vertical load predicted by Mod-MIXDYN (MIE).

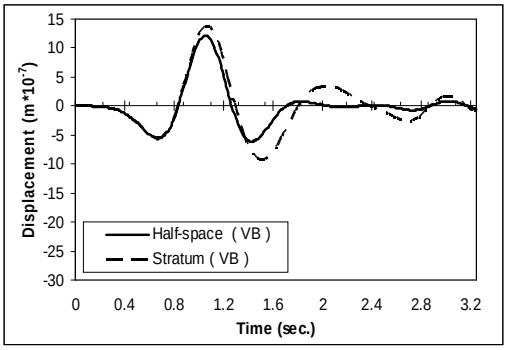

Fig. (17): Time history of horizontal displacements at point A due to vertical load predicted by ANSYS using (VB).

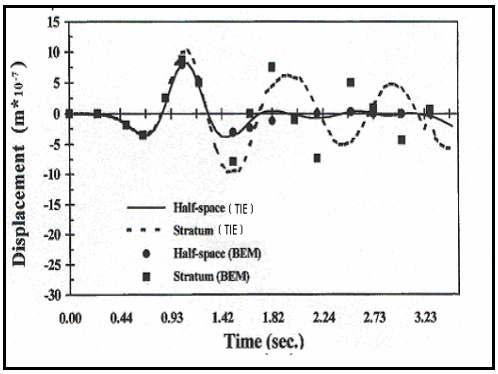

Fig. (18): Time history of horizontal displacements at point A due to vertical load, (Yerli et al., 1998)

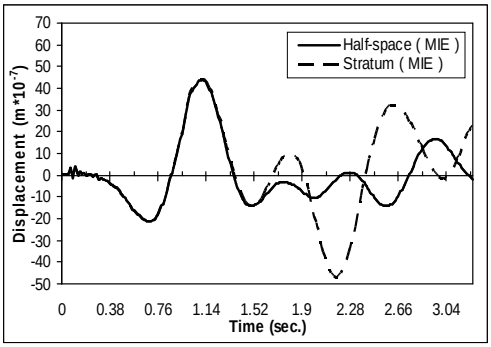

Fig. (19): Time history of horizontal displacements at point A due to horizontal load predicted by Mod-MIXDYN (MIE).

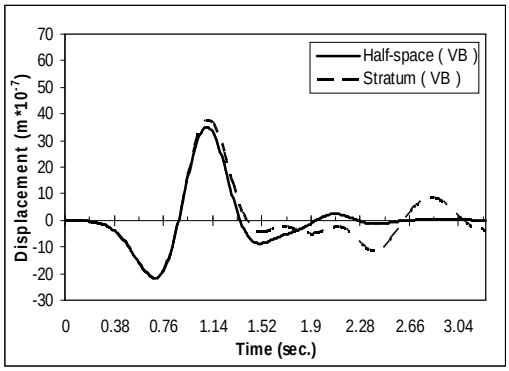

Fig. (20): Time history of horizontal displacements at point A due to horizontal load predicted by ANSYS using (VB).

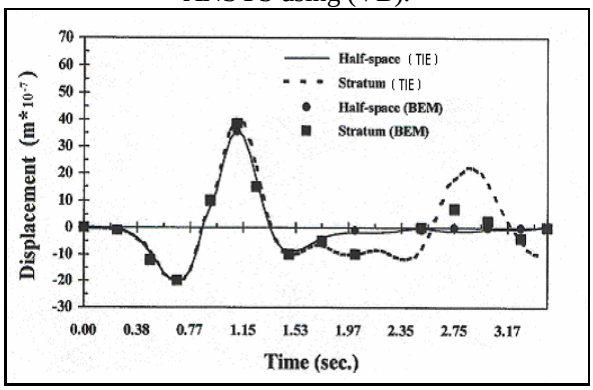

Fig. (21): Time history of horizontal displacements at point A due to horizontal load, (Yerli et al., 1998)

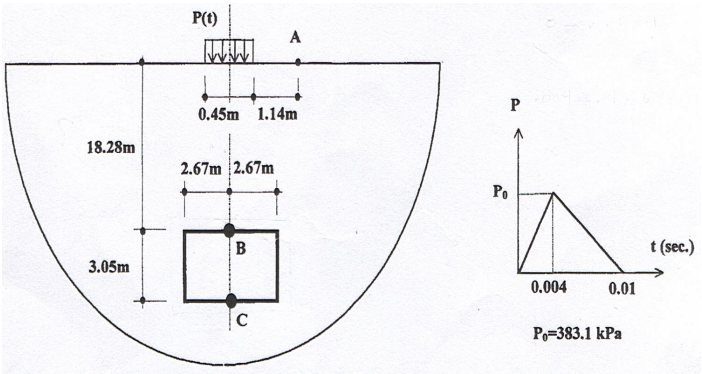

Fig. (22): Underground opening and forcing function of problem No. (2).

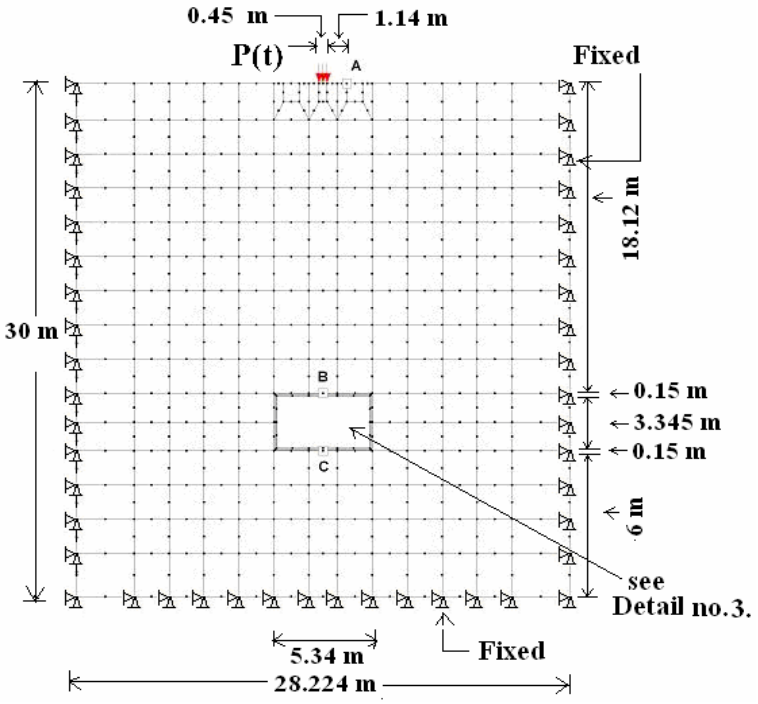

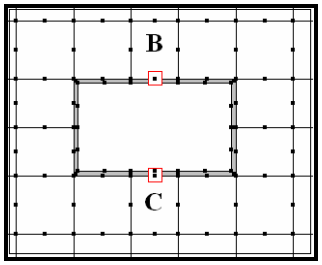

Fig.(23): Finite element mesh with fixed boundaries for problem No.(2).

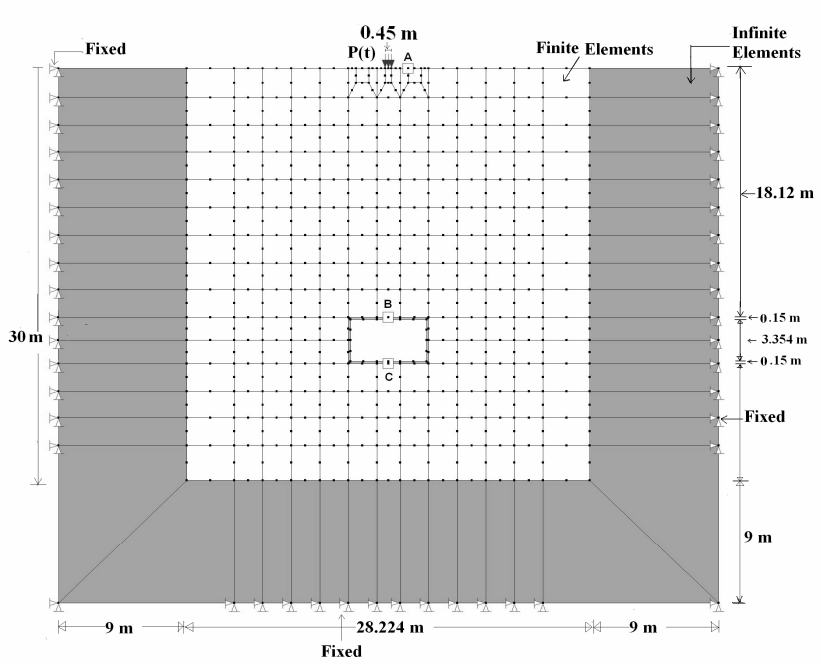

Fig.(24): Finite and infinite elements mesh for problem No. (2).

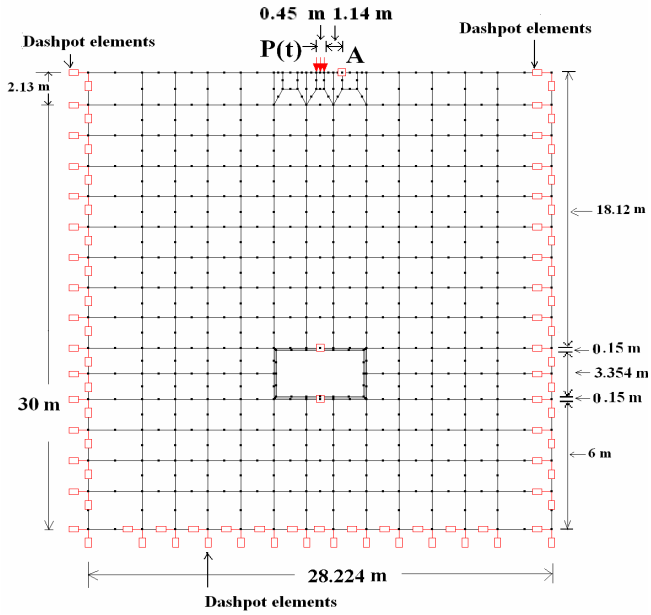

Fig. (25): Finite and dashpot elements mesh for problem No. (2).

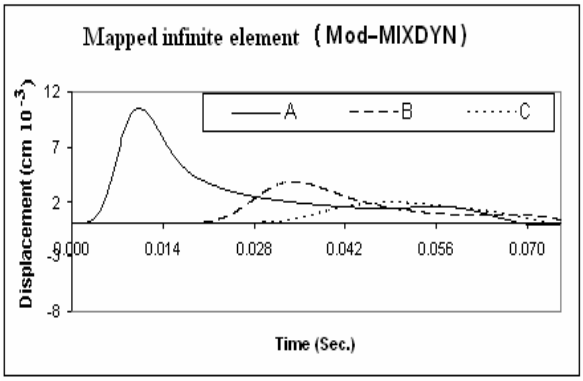

Fig. (26): Displacement versus time at points A, B and C using mapped infinite element (MIE) as predicted by (Mod-MIXDYN).

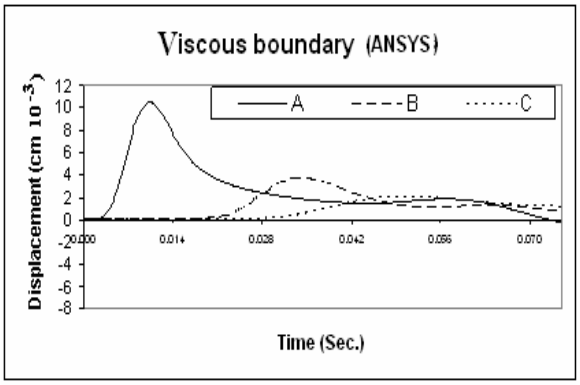

Fig. (27): Displacement versus time at points A, B and C considering viscous boundary (VB) as predicted by (ANSYS).

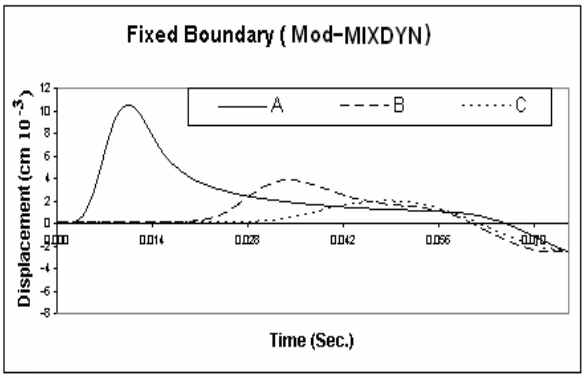

Fig. (28): Displacement versus time at points A, B and C considering fixed boundaries as predicted by (Mod-MIXDYN).

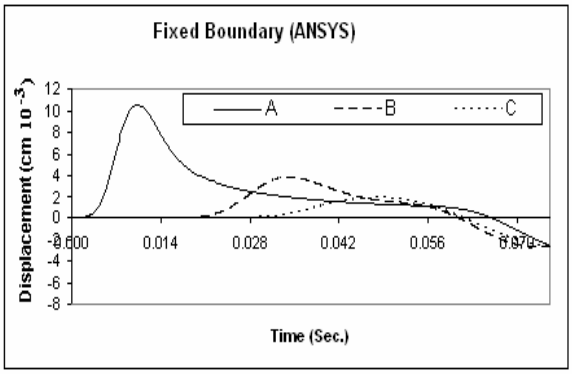

Fig. (29): Displacement versus time at points A, B and C considering fixed boundaries as predicted by (ANSYS).

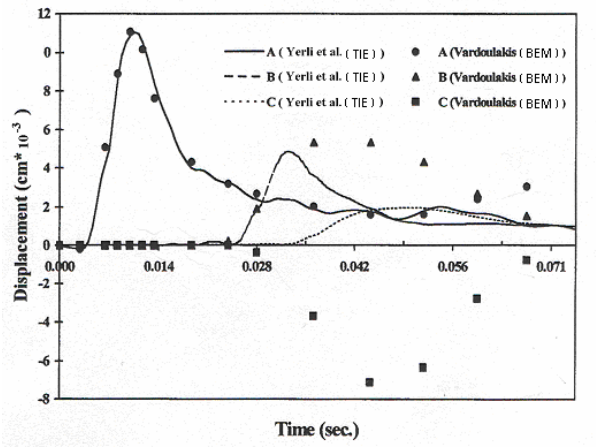

Fig. (30): Displacement versus time at points A, B and C using transient infinite elements, (Yerliet al., 1998)

عنصر غير محدد معين جديد للتحليل الديناميكي لمسائل التداخل بين التربة و المنشات

د. محمد يوسف فتاح

استاذ مساعد

قسم هندسة البناء والإنشاءات, الجامعة التكنولوجية

الخلاصة:

في الحسابات العددية يتم عادة تحليل منطقة محددة حول الأساس. و ما لم تتخذ اجراءات معينة لمنع الموجات المنتشرة من الأساس من الارتداد نتيجة الاصطدام بحدود المسألة يمكن أن تحدث أخطاء في النتائج. ان العمل الحالي يدرس هذه التأثيرات باستعمال طريقة العناصر المحددة مع نوعين من الحدود الناقلة عند حافات المسألة. النوع الأول عنصر غير محدد معين و الثاني باستعمال الحدود اللزجة. تم اشتقاق نوعين من العناصر غير المحددة هما العنصر غير المحدد ثماني العقد الذي يمثل امتدادا لعنصر Zienkiewicz غير المحدد و العنصر خماسي العقد غير المحدد المقدم من قبل Selvadurai and Karpurapu عام 1988. تم عرض دوال التعيين و مشتقاتها للعناصر غير المحددة لحالتين: الأولى عندما يكون العنصر غير المحدد ممتدا للمالانهاية في الاتجاه السالب ξ و الثاني عندما يكون العنصر ممتدا للمالانهاية بالاتجاه السالب η .

أجري تحليل بطريقة العناصر المحددة لمسائل التداخل بين التربة و المنشات اخذين بنظر الاعتبار الحدود الناقلة. و تم اعتبار نوعين من الحدود: الحدود اللزجة و العناصر غير المحددة المعينة. و تمت مقارنة النتائج لثلاث حالات: الأولى عند استعمال عناصر محددة لوحدها و الثانية باستعمال عناصر غير محددة معينة خماسية و ثمانية العقد و التي أضيفت الى برنامج الحاسبة MIXDYN و الحالة الثالثة باستعمال حدود لزجة.

و لغرض التحقق من صلاحية و دقة العناصر غير المحددة المشتقة في تحليل مسائل التداخل بين التربة و المنشات التي تأخذ بالاعتبار الحدود اللامنتهية تم تحليل مثالين لهذا الغرض. و قد قورنت نتائج البرنامج المطور مع نتائج برنامج حاسبة اخر يدعى ANSYS يتبنى نوعا اخر من التمثيل للحدود باستعمال الحدود اللزجة. و قد وجد أن الحدود اللزجة أكثر فعالية في امتصاص الموجات الناتجة عن الأحمال الديناميكية من العناصر غير المحددة المعينة و هذا يبدو واضحا عند مقارنة نتائج النوعين من العناصر مع العناصر غير المحددة الوقتية أو العابرة.

مفاتيح الدالة: داينميكي, التاثير المتبادل للتربة-المنشاء- العناصر المحددة-العناصر الغير المحددة.